Enhanced PUMA for Direction-of-arrival Estimation and its Performance Analysis

Cheng Qian, *Student Member, IEEE*, Lei Huang, *Senior Member, IEEE*, N. D. Sidiropoulos, *Fellow, IEEE* and H. C. So, *Fellow, IEEE*

***Abstract*—Direction-of-arrival (DOA) estimation is a problem of significance in many applications. In practice, due to the occurrence of coherent signals and/or when the number of available snapshots is small, it is a challenge to find DOAs accurately. This problem is revisited here through a new *enhanced principal-singular-vector utilization for modal analysis (EPUMA)* DOA estimation approach, which improves the threshold performance by first generating $(P+K)$ DOA candidates for K sources where $P \geq K$, and then judiciously selecting K of them. The asymptotic variance of EPUMA is theoretically derived, and numerical results are provided to validate the asymptotic analysis and illustrate the practical merits of EPUMA.**

***Index Terms*—DOA estimation, weighted least squares, linear prediction, subspace method, small sample size.**

I. Introduction

SUBSPACE based direction-of-arrival (DOA) estimation algorithms offer a good compromise between estimation accuracy and computational complexity. Due to their competitive advantages, subspace algorithms such as MUSIC [1]-[3] and ESPRIT [4]-[6] have been deeply studied during the past three decades, towards improving their so-called threshold performance and achieving high estimation accuracy, especially under certain challenging scenarios, such as in the sample-starved regime where relatively few snapshots are available, and in the case of correlated or even fully coherent signals.

The threshold effect refers to the severe and abrupt performance degradation that happens when the signal-to-noise ratio (SNR) and/or the sample size drops below a certain threshold, and it is the characteristic of many subspace based algorithms. At low SNR, this phenomenon can be alleviated by collecting a larger number of samples, but this is not always possible, especially in rapidly time-varying scenarios. To improve the threshold performance, pseudo-noise resampling (PR) strategies have been developed for maximum likelihood (ML) [7], unitary root-MUSIC [8], and unitary ESPRIT [9], where the received data is resampled several times by directly adding man-made noise. PR based algorithms use sectors determined via conventional beamforming techniques, and if a source DOA falls outside its presumed sector then they fall apart.

In recent work [10], the authors have studied the performance breakdown at the threshold SNR, and concluded that it is mainly due to the subspace leakage where the estimated signal subspace is corrupted by a portion of its orthogonal projection space. In order to improve the threshold performance, they proposed two algorithms named *root-swap root-MUSIC* and *two-step root-MUSIC*, where the former takes a different approach to determining the signal roots and the latter employs a modified sample covariance matrix (SCM) to estimate DOAs. Specifically, unlike conventional root-MUSIC, which picks the roots that are closest to the unit circle, the two-step root-MUSIC picks the roots that minimize the stochastic ML cost function (among those inside the unit circle). Note that using the ML cost function to determine final DOA estimates was first introduced in [11]. However, the performance of two-step root-MUSIC hinges on the modified SCM which is estimated by a time consuming one-dimensional search strategy. Furthermore, its high-SNR performance is limited by that of root-MUSIC, since the modified SCM is almost the same as the conventional SCM in this region. Therefore, in the presence of coherent signals (especially for closely-spaced DOAs), the performance of both root-swap and two-step root-MUSIC may not be satisfactory.

In the case of coherent signals, most of the subspace based estimators can be modified by some decorrelation techniques, e.g., spatial smoothing (SS) [12] and forward-backward spatial smoothing (FBSS) [13] methods. However, both of them have the drawback that decorrelation is achieved at the expense of reducing the array aperture, resulting in reduced degrees-of-freedom (DOF), which directly affects the DOA resolution performance. Generally speaking, smaller DOF will cause worse threshold performance. Thus, how to design DOA estimation algorithms that are able to deal with coherent signals has been an important problem in array signal processing.

Recently, an accurate and low-complexity algorithm called principal-singular-vector utilization for modal analysis (PUMA) has been proposed for frequency estimation [14]-[16]. However, in the low SNR and small sample (e.g., the sample size is smaller than the number of sources) regime, the PUMA method suffers performance breakdown which is mainly due to the outliers caused by the inaccurate estimation of the signal subspace, and such a performance degradation will be further aggravated if there are highly correlated or even coherent signals. To alleviate the aforementioned problems, motivated by the PUMA method for multiple sinusoids [16]

C. Qian and L. Huang are with the College of Information Engineering, Shenzhen University, Shenzhen, 518060 China (e-mail: qianc@umn.edu, dr.lei.huang@ieee.org).

N. D. Sidiropoulos is with the Department of Electronics and Computer Engineering, University of Minnesota Twin City, Minneapolis, 55455 United States (e-mail: nikos@umn.edu).

H. C. So is with the Department of Electronic Engineering, City University of Hong Kong, Hong Kong (e-mail: hcso@ee.cityu.edu.hk).

This research has been supported in part by Natural Science Foundation of China (NSFC) under Grant No. U1501253 and the Chinese Scholarship Council.

and also drawing insights from the two-step root-MUSIC method in [10], we propose an enhanced PUMA (EPUMA) algorithm which first generates $(P+K)$ DOA candidates where $P > K$, and then selects K of them using the deterministic ML criterion, to improve the threshold performance of PUMA. Using a uniform linear array (ULA), the DOA estimation problem can be formulated as a linear prediction (LP) problem [17]-[19] where the LP coefficients are estimated via an iteratively weighted least squares (WLS) technique. Furthermore, a detailed derivation of the asymptotic performance analysis of the EPUMA technique is presented. We theoretically prove that when there is only one source, the asymptotic variance is identical to the Cramér-Rao bound (CRB) in the high SNR case.

The rest of the paper is organized as follows. In Section II, we introduce the data model. In Section III, the EPUMA algorithm is derived. Section IV is devoted to analyze its asymptotic performance. In Section V, numerical simulations are provided to compare the performance of EPUMA with that of the deterministic ML, root-swap root-MUSIC, two-step root-MUSIC, and ESPRIT algorithms. Finally, conclusions are drawn in Section VI.

II. Signal Model

Consider a ULA with M isotropic sensors. There are K $(K < M)$ narrowband source signals impinging on the array from distinct directions $\{\theta_1, \cdots, \theta_K\}$ in the far field. The $M \times 1$ observation vector is

$$\mathbf{x}(t) = \mathbf{A}\mathbf{s}(t) + \mathbf{n}(t), \quad t = 1, \cdots, N. \tag{1}$$

Here, $\mathbf{A} = [\mathbf{a}(\theta_1) \ \cdots \ \mathbf{a}(\theta_K)]$ is the steering matrix, $\mathbf{s}(t) = [s_1(t) \ \cdots \ s_K(t)]^T$ is the source signal vector with $(\cdot)^T$ being the transpose, N is the number of snapshots, and the steering vector due to the kth source is expressed as

$$\mathbf{a}(\theta_k) = \left[1 \ e^{j2\pi \sin(\theta_k) d/\nu} \ \cdots \ e^{j2\pi(M-1)\sin(\theta_k)d/\nu}\right]^T \tag{2}$$

where ν is the carrier wavelength and $d = \nu/2$ is the inter-element spacing. It is assumed that the noise vector $\mathbf{n}(t)$ is a white Gaussian process with mean zero and covariance $\sigma_n^2 \mathbf{I}_M$ where σ_n^2 is the power and $\mathbf{I}_M$ is the $M \times M$ identity matrix. Moreover, the noise is uncorrelated with $\mathbf{s}(t)$. Our task is to estimate the K DOAs from the observations $\{\mathbf{x}(t)\}_{t=1}^N$. The covariance matrix of $\mathbf{x}(t)$ is

$$\mathbf{R} = \mathbb{E}[\mathbf{x}(t)\mathbf{x}^H(t)] = \mathbf{A}\mathbf{R}_s\mathbf{A}^H + \sigma_n^2 \mathbf{I}_M \tag{3}$$

where $\mathbb{E}[\cdot]$ denotes expectation, $(\cdot)^H$ is the conjugate transpose, and $\mathbf{R}_s = \mathbb{E}[\mathbf{x}(t)\mathbf{x}^H(t)]$ denotes the signal covariance matrix.

Note that, throughout the paper, the number of sources K is assumed to be known. For detecting the number of sources, Akaike's information criterion (AIC) [20] and minimum description length (MDL) [21] are the most widely studied algorithms. Interested readers are referred to [22]-[24], where scenarios involving small number of samples and coherent sources are considered.

III. EPUMA Algorithm

A. PUMA with Extra DOA Estimates

Define the eigenvalue decomposition (EVD) of $\mathbf{R}$ as

$$\mathbf{R} = \mathbf{U}_s\mathbf{\Lambda}_s\mathbf{U}_s^H + \sigma_n^2\mathbf{U}_n\mathbf{U}_n^H \tag{4}$$

where $\mathbf{U}_s = [\mathbf{u}_1 \ \cdots \ \mathbf{u}_K]$ is the signal subspace, $\mathbf{U}_n = [\mathbf{u}_{K+1} \ \cdots \ \mathbf{u}_M]$ is the noise subspace and $\mathbf{\Lambda}_s = \text{diag}(\lambda_1 \ \cdots \ \lambda_K)$ that contains the K largest eigenvalues with $\lambda_1 \geq \cdots \geq \lambda_K \geq \sigma_n^2$, $\{\mathbf{u}_i\}_{i=1}^K$ being its corresponding signal eigenvectors and $\{\mathbf{u}_i\}_{i=K+1}^M$ being the noise eigenvectors. Here, $\text{diag}(\cdot)$ denotes a diagonal matrix.

In the ideal case where $\mathbf{R}$ is exactly known, $\mathbf{U}_s$ and $\mathbf{A}$ span the same column space

$$\text{span}(\mathbf{U}_s) = \text{span}(\mathbf{A}). \tag{5}$$

Since $\mathbf{A}$ is a Vandermonde matrix, according to the LP theory, each column of $\mathbf{U}_s$ is a sum of $P \in [K, M-1]$ sinusoids. More precisely, each element in $\mathbf{u}_k$ can be expressed as a linear combination of its previous P samples [16]:

$$[\mathbf{u}_k]_m = -\sum_{i=1}^{P} c_i [\mathbf{u}_k]_{m-i}, \quad k = 1, \cdots, K, \ m = P+1, \cdots, M \tag{6}$$

where $[\mathbf{u}_k]_m$ is the mth element in $\mathbf{u}_k$ and $\{c_i\}_{i=1}^P$ are the LP coefficients. Therefore, the DOAs θ_k can be related to the following polynomial [25]

$$z_k^P + \sum_{i=1}^{P} c_i z_k^{P-i} = 0 \tag{7}$$

where $z_k = e^{j2\pi \sin(\theta_k)d/\nu}$, $k = 1, \cdots, K$.

The matrix form of (6) is

$$\mathbf{F}_k\mathbf{c} - \mathbf{g}_k = \mathbf{0}_{M-P} \tag{8}$$

where $\mathbf{0}_{M-P}$ is a $(M-P) \times 1$ zero vector, and

$$\mathbf{F}_k = \begin{bmatrix} [\mathbf{u}_k]_P & [\mathbf{u}_k]_{P-1} & \cdots & [\mathbf{u}_k]_1 \\ [\mathbf{u}_k]_{P+1} & [\mathbf{u}_k]_P & \cdots & [\mathbf{u}_k]_2 \\ \vdots & \vdots & & \vdots \\ [\mathbf{u}_k]_{M-1} & [\mathbf{u}_k]_{M-2} & \cdots & [\mathbf{u}_k]_{M-P} \end{bmatrix} \tag{9}$$

$$\mathbf{c} = [c_1 \ \cdots \ c_P]^T \tag{10}$$

$$\mathbf{g}_k = -[[\mathbf{u}_k]_{P+1} \ \cdots \ [\mathbf{u}_k]_M]^T. \tag{11}$$

Let $\mathbf{e}_k = \mathbf{F}_k\mathbf{c} - \mathbf{g}_k$. Stacking $\{\mathbf{e}_k\}_{k=1}^K$ into a vector yields

$$\begin{aligned} \mathbf{e} &= [\mathbf{e}_1^T \ \cdots \ \mathbf{e}_K^T]^T \\ &= \mathbf{F}\mathbf{c} - \mathbf{g} = \mathbf{0}_{(M-P)K} \end{aligned} \tag{12}$$

where

$$\mathbf{F} = [\mathbf{F}_1^T \ \cdots \ \mathbf{F}_K^T]^T \tag{13}$$

$$\mathbf{g} = [\mathbf{g}_1^T \ \cdots \ \mathbf{g}_K^T]^T. \tag{14}$$

However, the covariance $\mathbf{R}$ is not available in practice. The typical approach is to use the sample covariance matrix $\hat{\mathbf{R}}$ instead of $\mathbf{R}$ where

$$\hat{\mathbf{R}} = \frac{1}{N}\mathbf{X}\mathbf{X}^H \tag{15}$$

with $\mathbf{X} = [\mathbf{x}(1) \ \cdots \ \mathbf{x}(N)]$ being the data matrix[1]. Take the EVD of $\hat{\mathbf{R}}$ as

$$\hat{\mathbf{R}} = \hat{\mathbf{U}}_s \hat{\mathbf{\Lambda}}_s \hat{\mathbf{U}}_s^H + \hat{\mathbf{U}}_n \hat{\mathbf{\Lambda}}_n \hat{\mathbf{U}}_n^H \tag{16}$$

where

$$\hat{\mathbf{U}}_s = [\hat{\mathbf{u}}_1 \ \cdots \ \hat{\mathbf{u}}_K] \tag{17}$$
$$\hat{\mathbf{U}}_n = [\hat{\mathbf{u}}_{K+1} \ \cdots \ \hat{\mathbf{u}}_M] \tag{18}$$
$$\hat{\mathbf{\Lambda}}_s = \text{diag}(\hat{\lambda}_1 \ \cdots \ \hat{\lambda}_K) \tag{19}$$
$$\hat{\mathbf{\Lambda}}_n = \text{diag}(\hat{\lambda}_{K+1} \ \cdots \ \hat{\lambda}_M). \tag{20}$$

In the presence of noise, we replace $\mathbf{u}_k$ by $\hat{\mathbf{u}}_k$ in (12) and produce $\hat{\mathbf{F}}$ and $\hat{\mathbf{g}}$. Thus, (12) becomes an approximate equality, i.e.,

$$\hat{\mathbf{F}}\mathbf{c} \approx \hat{\mathbf{g}}. \tag{21}$$

The straightforward way to estimate $\mathbf{c}$ is to utilize least squares (LS). However, the LS technique is suboptimal since both sides of (21) contain noise (due to the estimation errors). For this reason, we employ WLS instead of LS to estimate $\mathbf{c}$. The use of WLS in this context is called weighted linear prediction, and it has been successfully used in other signal processing applications, where it was shown to yield a significant improvement in the estimation performance [26]-[27]. The WLS technique tries to minimize the following cost function

$$\hat{\mathbf{e}}^H \mathbf{W} \hat{\mathbf{e}} \tag{22}$$

where

$$\hat{\mathbf{e}} = \hat{\mathbf{F}}\mathbf{c} - \hat{\mathbf{g}} \tag{23}$$
$$\mathbf{W} = \left(\mathbb{E}\big[\hat{\mathbf{e}}\hat{\mathbf{e}}^H\big]\right)^{-1}. \tag{24}$$

The solution to the unconstrained minimization of (22) is

$$\hat{\mathbf{c}} = (\hat{\mathbf{F}}^H \mathbf{W} \hat{\mathbf{F}})^{-1} \hat{\mathbf{F}}^H \mathbf{W} \hat{\mathbf{g}}. \tag{25}$$

However, we cannot directly use (25) to estimate $\hat{\mathbf{c}}$ since $\mathbf{W}$ is the true covariance matrix of $\hat{\mathbf{e}}$ which is unavailable. The calculation of $\mathbf{W}$ requires knowledge of $\mathbf{c}$ and also both the signal eigenvalues $\lambda_1, \cdots, \lambda_K$, and the noise power σ_n^2. Despite all that it is still possible to calculate an approximate optimal weighting $\hat{\mathbf{W}}$ by substituting consistent estimates of $\mathbf{c}$, $\lambda_1, \cdots, \lambda_K$, and σ_n^2.

In the absence of noise, we find that

$$\mathbf{e}_k = \mathbf{B}(\mathbf{c})\mathbf{u}_k = \mathbf{0}_{M-P}, \ k = 1, \cdots, K \tag{26}$$

where

$$\mathbf{B}(\mathbf{c}) = \text{Toeplitz}\big([c_P \ \mathbf{0}_{M-P-1}^T]^T, [c_P \ \cdots \ c_1 \ 1 \ \mathbf{0}_{M-P-1}^T]\big) \in \mathbb{C}^{(M-P)\times M} \tag{27}$$

[1]In order to circumvent the problem of degraded estimation performance in case of closely-spaced DOAs in the same dimension, $\hat{\mathbf{R}}$ can be replaced by the forward-backward (FB) smoothing covariance matrix:

$$\hat{\mathbf{R}}_{\text{FB}} = \frac{1}{2}\big(\hat{\mathbf{R}} + \mathbf{\Pi}_M \hat{\mathbf{R}}^* \mathbf{\Pi}_M\big)$$

where $(\cdot)^*$ is the complex conjugate and $\mathbf{\Pi}_M$ is the $M \times M$ exchange matrix with ones on its anti-diagonal and zeros elsewhere.

where Toeplitz$(\mathbf{a}, \mathbf{b})$ stands for a Toeplitz matrix having $\mathbf{a}$ as its first column and $\mathbf{b}$ as its first row. Moreover, we have

$$\begin{aligned}\mathbf{e} &= \text{vec}([\mathbf{e}_1 \ \mathbf{e}_2 \ \cdots \ \mathbf{e}_K]) \\ &= \text{vec}(\mathbf{B}(\mathbf{c})\mathbf{U}_s) = \mathbf{0}_{(M-P)K}\end{aligned} \tag{28}$$

where vec$(\cdot)$ is the vectorization operator. By taking the noise into consideration, (28) becomes

$$\begin{aligned}\hat{\mathbf{e}} &= \text{vec}\Big(\mathbf{B}(\mathbf{c})\hat{\mathbf{U}}_s\Big) \\ &= \text{vec}\Big(\mathbf{B}(\mathbf{c})(\mathbf{U}_s + \Delta\mathbf{U}_s)\Big) \\ &= \text{vec}\Big(\mathbf{B}(\mathbf{c})\Delta\mathbf{U}_s\Big) \\ &= \big(\mathbf{I}_K \otimes \mathbf{B}(\mathbf{c})\big)\Delta\mathbf{u}_s\end{aligned} \tag{29}$$

where $\otimes$ is the Kronecker product, $\hat{\mathbf{U}}_s = \mathbf{U}_s + \Delta\mathbf{U}_s$, and $\Delta\mathbf{u}_s = \text{vec}(\Delta\mathbf{U}_s)$. According to (24), $\mathbf{W}$ has the form of

$$\begin{aligned}\mathbf{W} &= \mathbb{E}\big[\hat{\mathbf{e}}\hat{\mathbf{e}}^H\big]^{-1} \\ &= \Big[\big(\mathbf{I}_K \otimes \mathbf{B}(\mathbf{c})\big)\mathbb{E}\big[\Delta\mathbf{u}_s\Delta\mathbf{u}_s^H\big]\big(\mathbf{I}_K \otimes \mathbf{B}(\mathbf{c})\big)^H\Big]^{-1}.\end{aligned} \tag{30}$$

It is shown in [28]-[31] that the errors between the signal eigenvectors have the following property:

$$\mathbb{E}\big[\Delta\mathbf{u}_i\Delta\mathbf{u}_j^H\big] \approx \frac{\lambda_i}{N}\sum_{\substack{k=1\\k\neq i}}^{M}\frac{\lambda_k}{(\lambda_i-\lambda_k)^2}\mathbf{u}_k\mathbf{u}_k^H\delta_{ij} \tag{31}$$

where δ_{ij} is the delta function. It follows from (31) that

$$\mathbb{E}[\Delta\mathbf{u}_s\Delta\mathbf{u}_s^H] \approx \begin{bmatrix}\mathbb{E}[\Delta\mathbf{u}_1\Delta\mathbf{u}_1^H] & & \\ & \ddots & \\ & & \mathbb{E}[\Delta\mathbf{u}_K\Delta\mathbf{u}_K^H]\end{bmatrix}. \tag{32}$$

Since $(\mathbf{I}_K \otimes \mathbf{B}(\mathbf{c}))$ and $\mathbb{E}[\Delta\mathbf{u}_s\Delta\mathbf{u}_s^H]$ are all block diagonal matrices, $\mathbf{W}$ is also a block diagonal matrix where its ith diagonal matrix is

$$\mathbf{B}(\mathbf{c})\mathbb{E}[\Delta\mathbf{u}_i\Delta\mathbf{u}_i^H]\mathbf{B}^H(\mathbf{c}) \approx \frac{\lambda_i\sigma_n^2}{N(\lambda_i-\sigma_n^2)^2}\mathbf{B}(\mathbf{c})\mathbf{U}_n\mathbf{U}_n^H\mathbf{B}^H(\mathbf{c}). \tag{33}$$

Noting that $\mathbf{U}_n\mathbf{U}_n^H = \mathbf{I}_M - \mathbf{U}_s\mathbf{U}_s^H$ and utilizing the result in (28), (33) yields

$$\mathbf{B}(\mathbf{c})\mathbb{E}[\Delta\mathbf{u}_i\Delta\mathbf{u}_i^H]\mathbf{B}^H(\mathbf{c}) \approx \frac{\lambda_i\sigma_n^2}{N(\lambda_i-\sigma_n^2)^2}\mathbf{B}(\mathbf{c})\mathbf{B}^H(\mathbf{c}). \tag{34}$$

Combining (30), (32) and (34) yields

$$\mathbf{W} \approx \mathbf{\Gamma} \otimes \big(\mathbf{B}(\mathbf{c})\mathbf{B}^H(\mathbf{c})\big)^{-1}. \tag{35}$$

where

$$\mathbf{\Gamma} = \begin{bmatrix}\frac{N}{\sigma_n^2}\frac{(\lambda_1-\sigma_n^2)^2}{\lambda_1} & & \\ & \ddots & \\ & & \frac{N}{\sigma_n^2}\frac{(\lambda_K-\sigma_n^2)^2}{\lambda_K}\end{bmatrix}. \tag{36}$$

It is seen in (35) that there are three unknown components, namely, σ_n, λ_k and $\mathbf{c}$ in $\mathbf{W}$. For λ_k, one simple and straightforward way is to replace λ_k by $\hat{\lambda}_k$. For σ_n^2, we replace it by its consistent estimate which is given by [32]

$$\hat{\sigma}_n^2 = \frac{1}{M-K}\text{tr}(\hat{\mathbf{\Lambda}}_n) \tag{37}$$

where $\mathrm{tr}(\cdot)$ is the trace of a matrix. We note that when $N \leq K$, $\hat{\mathbf{\Lambda}}_n$ becomes a zero matrix. Thus, we have $\hat{\sigma}_n^2 = 0$. However, if $\hat{\sigma}_n^2 = 0$, $\mathbf{\Gamma}$ in (36) will be infinity that makes $\mathbf{W}$ ill-conditioned. Nevertheless, it is easily seen from (25) that N/σ_n^2 will be canceled out and thus it can be ignored. Finally, we obtain the approximate optimal weighting $\hat{\mathbf{W}}$ as

$$\hat{\mathbf{W}} = \hat{\mathbf{\Gamma}} \otimes \left(\mathbf{B}(\mathbf{c})\mathbf{B}^H(\mathbf{c})\right)^{-1} \tag{38}$$

where

$$\hat{\mathbf{\Gamma}} = \begin{bmatrix} \frac{(\hat{\lambda}_1 - \hat{\sigma}_n^2)^2}{\hat{\lambda}_1} & & \\ & \ddots & \\ & & \frac{(\hat{\lambda}_K - \hat{\sigma}_n^2)^2}{\hat{\lambda}_K} \end{bmatrix}. \tag{39}$$

At this point, the original WLS problem in (22) is approximated by

$$\hat{\mathbf{c}} = \arg\min_{\mathbf{c}} \ \hat{\mathbf{e}}^H \hat{\mathbf{W}} \hat{\mathbf{e}} \tag{40}$$

whose solution is

$$\hat{\mathbf{c}} = (\hat{\mathbf{F}}^H \hat{\mathbf{W}} \hat{\mathbf{F}})^{-1} \hat{\mathbf{F}}^H \hat{\mathbf{W}} \hat{\mathbf{g}}. \tag{41}$$

We should point out that the DOA estimation accuracy depends on how accurate $\hat{\mathbf{c}}$ is. However, note from (41) that $\hat{\mathbf{c}}$ is not available at this time since $\mathbf{B}(\mathbf{c})$ is unknown. Thus, our next goal is to find a proper way to approximate $\mathbf{B}(\mathbf{c})$. Towards this end, we suggest using the LS estimate from (21), namely

$$\hat{\mathbf{c}}_{\text{LS}} = \hat{\mathbf{F}}^{\dagger} \hat{\mathbf{g}} \tag{42}$$

where $(\cdot)^{\dagger}$ is the pseudo-inverse. This enables us to initialize $\mathbf{B}(\mathbf{c})$ by substituting (42) into (27), leading to

$$\hat{\mathbf{W}}_{\text{init}} = \hat{\mathbf{\Gamma}} \otimes \left(\mathbf{B}(\hat{\mathbf{c}}_{\text{LS}})\mathbf{B}^H(\hat{\mathbf{c}}_{\text{LS}})\right)^{-1}. \tag{43}$$

Then plugging (43) into (41) produces a new estimate of $\mathbf{c}$. The latter can also be exploited to update $\hat{\mathbf{W}}$ and thus obtain an improved estimate of $\mathbf{c}$. Such an iterative estimation procedure can be summarized as follows:

1) Initialize $\mathbf{B}(\mathbf{c})$ by using $\hat{\mathbf{c}}_{\text{LS}}$ in (42);
2) Utilize the obtained $\mathbf{B}(\mathbf{c})$ to construct $\hat{\mathbf{W}}$ via (38);
3) Calculate $\hat{\mathbf{c}}$ via (41);
4) Repeat 2) to 3) until a stopping criterion is satisfied[2].

After obtaining $\hat{\mathbf{c}}$ and solving for the P roots, denoted by $\{\hat{z}_i\}$, we get a total of P DOA candidates, i.e.,

$$\hat{\theta}_i = \sin^{-1}\left(\frac{\nu \angle \hat{z}_i}{2\pi d}\right), \ i = 1, \cdots, P. \tag{44}$$

When there are $P > K$ DOA candidates, the question that naturally arises is what criterion should be used to reduce them down to K final DOA estimates.

[2]Two or three iterations are enough in most cases for EPUMA to achieve reliable performance, and further iterations do not bring any significant performance improvement, in our experience. We therefore stop iterating after a fixed number of iterations in our simulations.

B. Two-Step DOA Selection Strategy

Contrary to 'conventional wisdom', we *do not* advocate determining the K DOA estimates by choosing the K signal roots that are closest to the unit circle. There are mainly two reasons against this: 1) In low SNR cases, especially when the signal power is smaller than the noise power, there is a high probability of subspace leakage [10], i.e., the noise perturbation occupies some portion in the signal subspace resulting in $(P - K)$ noise rooting, since signal roots have smaller amplitudes than the noise roots; and 2) Through empirical and theoretical study, we find that for the PUMA, a larger P, namely, $P > K$, usually produces better threshold performance than the case of $P = K$ but the latter possesses higher estimation accuracy than the former when SNR is high or the sample size is large. For 1), we follow [10] to make use of a larger sized LP system to produce $P > K$ DOA candidates, and then determine the final K DOA estimates from the P DOA candidates. For 2), since the signal subspace contains a large portion of its null space for low SNRs, the K signal roots of the PUMA with $P = K$ are corrupted by those from the null space. Unfortunately, the PUMA algorithm will treat them as the signal roots, resulting in some unreliable DOA estimates and thus leading to significant performance degradation. However, for the case of $P > K$, the PUMA will generate more than K signal root candidates. This increases the probability of removing the outliers and finding K DOA estimates associated with the true DOAs at the same time. Nevertheless, P cannot be too large, because a larger P produces a smaller dimension of $\mathbf{F}_k$ and leads to smaller DOF. In this way, the root mean square error (RMSE) curve of PUMA will depart from the CRB as P increases.

This intuition will be confirmed by our theoretical performance analysis, but before we get to that, it is instructive to illustrate this point by means of examples. We consider a 10-element ULA receiving two correlated source signals from $\theta_1 = -2^\circ$ and $\theta_2 = 4^\circ$. We choose $P = K$, $K+1$, $K+2$ and $K+3$ for comparison. In the first example, we set $N = 2$ and SNR$= 0$ dB. Fig. 1 plots the the magnitude of the P estimated signal root candidates versus their corresponding DOA estimates. It is seen that the PUMA with $P = K$ only has one DOA estimate close to the true one while another one is far away from 2°. Moreover, the criterion that chooses the K signal roots that are closest to the unit circle is inappropriate. Taking $P = K + 2$ as an example, the second and third roots are the correct ones, but, according to that criterion, we should choose the second and fourth roots as signal roots.

In the second example, we set the sample size as $N = 40$ and include the CRB [33] as a benchmark, and a preview of the analytical variance expression in (47). A total of 2000 Monte Carlo tests are carried out to compute the RMSE, where

$$\text{RMSE} = 10\log_{10}\sqrt{\frac{1}{2000K}\sum_{k=1}^{K}\sum_{i=1}^{2000}(\hat{\theta}_{k,i} - \theta_k)^2}. \tag{45}$$

Note that the final DOA estimates are determined by the second step. The only difference is that we generate $\binom{P}{K}$ candidate subsets of K DOAs each, and then employ the ML cost function in (46) to determine the final K DOA estimates.

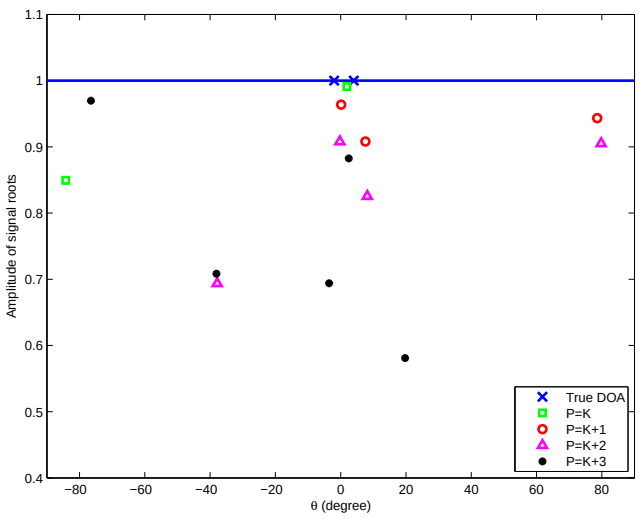

Fig. 1. Root radii of PUMA with $P = K, K+1, K+2, K+3$ when $N = 2$ and two coherent signals with $\theta = [-2°, 4°]$

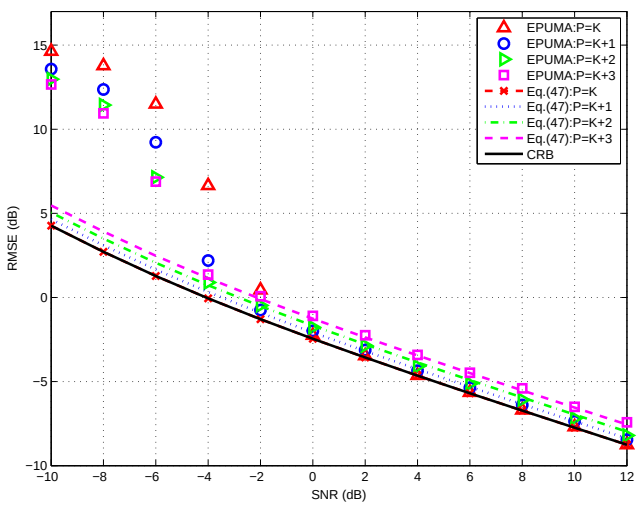

Fig. 2. RMSE performance of PUMA for different P versus SNR when $N = 40$ and two coherent signals with $\theta = [-2°, 4°]$

It is shown in Fig. 2 that a larger P provides better threshold performance but with a little bit larger variance in the high SNR regime.

From the above discussion and 'sneak preview', we find that to improve the threshold performance, it is better to choose $P > K$, while to decrease the variance in the high SNR region, it is preferable to use $P = K$. This suggests the following two-step idea, i.e., the *EPUMA algorithm*:

i) Employ the PUMA twice with $P = K$ and $P > K$, respectively, to generate $(K + P)$ DOA candidates;
ii) Pick up K DOA estimates from the estimated $(K + P)$ DOA candidates.

For Step ii), in order to reliably choose K DOA estimates, we follow [10]-[11] to determine the final DOAs:

1) Divide all the $(P+K)$ DOAs into $G = \frac{(P+K)!}{K!P!}$ different subsets with each subset having K different DOAs, denoted by $\Theta_1, \cdots, \Theta_G$, which corresponds to G different $\mathbf{A}$, i.e., $\mathbf{A}(\Theta_1), \cdots, \mathbf{A}(\Theta_G)$;
2) Substitute each $\mathbf{A}(\Theta_i)$ into the ML cost function[3]
$$L(\Theta) = \mathrm{tr}\big((\mathbf{I}_M - \mathbf{A}(\Theta)(\mathbf{A}^H(\Theta)\mathbf{A}(\Theta))^{-1}\mathbf{A}^H(\Theta))\hat{\mathbf{R}}\big) \tag{46}$$
which yields $L(\Theta_1), \cdots, L(\Theta_G)$.
3) The final DOAs are in the $\Theta_I, I \in \{1, \cdots, G\}$ that minimizes $L(\Theta)$ among all those considered.

Remark 1: The implementation of the EPUMA algorithm requires three major steps:

1) Calculation of $\hat{\mathbf{R}}$ and its EVD;
2) Inversion of $\hat{\mathbf{W}}$;
3) Calculation of $\hat{\mathbf{c}}$.

The total flops to calculate $\hat{\mathbf{R}}$ is about $\mathcal{O}(M^2N)$, while the complexity for its EVD is $\mathcal{O}(M^3)$. Since $\hat{\mathbf{W}}$ is a block diagonal matrix, the computational complexity of $\hat{\mathbf{W}}^{-1}$ is mainly caused by the inverse of $\big(\mathbf{B}(\hat{\mathbf{c}}_{\mathrm{LS}})\mathbf{B}^H(\hat{\mathbf{c}}_{\mathrm{LS}})\big)$ which is about $\mathcal{O}((M-P)^3)$, and thus the computation of $\hat{\mathbf{W}}^{-1}$ is about $\mathcal{O}(K(M-P)^3)$. The complexity of calculating $\hat{\mathbf{c}}$ is about $\mathcal{O}(2P^2K(M-P)+2PK(M-P)^2+P^3+PK(M-P))$. Recalling that the EPUMA is implemented twice to generate $(P+K)$ DOA candidates, in each iteration, $\hat{\mathbf{c}}$ and $\hat{\mathbf{W}}$ are calculated two times. Moreover, the complexity for the final DOA selection is $\mathcal{O}(G(M^3 + 3MK^2 + K^3))$. Since P is usually a little bit larger than K, e.g., $P = K+1$ or $P = K+2$, by considering $P \approx K$, the complexity of the EPUMA scheme is about $\mathcal{O}(M^3 + M^2N + I(M^3 - K^3 - 11MK^2 - 2M^2K + 4K^3M + 4K^2M^2) + G(M^3 + 3MK^2 + K^3))$ with I being the number of iterations. As a matter of fact that $I = 2$ is enough for the EPUMA to achieve comparable performance, thus, we have $G \gg I$. If $M \gg K$, the complexity is reduced to $\mathcal{O}(M^2N + GM^3)$.

IV. Performance Analysis

A. Mean Square Error Analysis

It is often interesting and meaningful to know the quality of an estimator. The asymptotic performance of PUMA methods for one- and two-dimensional frequency estimation of a single-tone has been recently studied in the literature [15]-[16]. However, the performance analysis of PUMA for multiple frequencies has not yet been analyzed. In this section, under a high SNR assumption and using first- and second-order approximations, a *closed-form* variance expression for the EPUMA algorithm for DOA estimation is derived. The main result is summarized in the following proposition.

Proposition 1: The asymptotic variance of the PUMA algorithm in Section III-A for DOA estimation is[4]

[3]Although we employ the determined ML cost function as a criterion for final DOA selection, the readers can also use the stochastic one. However, from numerical simulations, we find that compared to the determined ML criterion, there is little threshold performance improvement when we employ the stochastic one, and sometimes the former is even better than the latter. Besides this, the stochastic ML cost function has higher complexity than the determined one. Therefore, we recommend to use the determined ML cost function to determine the final DOA estimates.

[4]Note that the true LP coefficients $\{c_i\}_{i=1}^P$ can be obtained by calculating the LS solution of (12), i.e., $\mathbf{c} = \mathbf{F}^\dagger\mathbf{g}$. When $P = K$, we can also compute $\mathbf{c}$ by forming the following polynomial
$$(z - e^{j2\pi d\sin(\theta_1)/\nu}) \times \cdots \times ((z - e^{j2\pi d\sin(\theta_K)/\nu})) = 0.$$

$$\mathbb{E}[(\Delta\theta_i)^2] \approx \frac{1}{2}\left(\frac{\nu}{2\pi d\cos(\theta_i)}\right)^2 \mathbb{E}\big[|\Delta z_i|^2\big] \tag{47}$$

where $|\cdot|$ is the absolute value and

$$\mathbb{E}\big[|\Delta z_i|^2\big] \approx \frac{\mathbf{z}_i^T\big(\mathbf{F}^H\mathbf{W}\mathbf{F}\big)^{-1}\mathbf{z}_i^*}{|\alpha_i|^2} \tag{48}$$

with

$$\mathbf{z}_i = [z_i^{P-1} \ \cdots 1]^T \tag{49}$$

$$\alpha_i = Pz_i^{P-1} + (P-1)c_1 z_i^{P-2} + \cdots + c_{P-1}. \tag{50}$$

Proof: See Appendix A. ■

Remark 2: It should be pointed out here that when $P > K$, Proposition 1 gives the asymptotic variance of PUMA for a single P rather than the two-step idea in Section III-B, where we combine two PUMA estimators with $P = K$ and $P > K$ to determine the final DOA estimates. For the latter, since (47) is established in the high SNR cases where the estimation accuracy only depends on PUMA with $P = K$, the asymptotic variance of EPUMA is exactly the variance of PUMA with $P = K$ which can be calculated via substituting $P = K$ into (47).

B. Special Case: Asymptotic Variance of EPUMA for a Single Source

In this case, there is only one vector in the signal subspace, i.e.,

$$\hat{\mathbf{U}}_s = \hat{\mathbf{u}}_1. \tag{51}$$

The $\mathbf{F}$ and $\mathbf{g}$ are reduced to

$$\hat{\mathbf{F}} = \hat{\mathbf{v}}_1 \tag{52}$$

$$\hat{\mathbf{g}} = \hat{\mathbf{v}}_2 \tag{53}$$

$$\mathbf{c} = c_1 \tag{54}$$

where

$$\hat{\mathbf{v}}_1 = \big[[\hat{\mathbf{u}}_1]_1 \ \cdots \ [\hat{\mathbf{u}}_1]_{M-1}\big]^T \tag{55}$$

$$\hat{\mathbf{v}}_2 = \big[[\hat{\mathbf{u}}_1]_2 \ \cdots \ [\hat{\mathbf{u}}_1]_{M}\big]^T \tag{56}$$

From the rotational invariance property, assuming that the noise is small, we have

$$\hat{\mathbf{v}}_2 \approx z\hat{\mathbf{v}}_1. \tag{57}$$

According to the definition of $\mathbf{B}(\mathbf{c})$ in (27), we find it can be expressed as

$$\mathbf{B}(c_1) = \text{Toeplitz}\left([c_1 \ \mathbf{0}_{M-2}^T]^T, [c_1 \ 1 \ \mathbf{0}_{M-2}^T]\right) \tag{58}$$

where $c_1 = -z$. Adopting the WLS approach for (57) produces

$$\begin{aligned}\hat{z} &= \arg\min_{\mathbf{z}} \ (\hat{\mathbf{v}}_2 - z\hat{\mathbf{v}}_1)^H\mathbf{T}(\hat{\mathbf{v}}_2 - z\hat{\mathbf{v}}_1)\\ &= \frac{\hat{\mathbf{v}}_1^H\mathbf{T}\hat{\mathbf{v}}_2}{\hat{\mathbf{v}}_1^H\mathbf{T}\hat{\mathbf{v}}_1}\end{aligned} \tag{59}$$

Thus, c_i associates with the coefficient of z^{K-i}.

where

$$\mathbf{T} = \frac{N(\lambda_1-\sigma_n^2)^2}{\lambda_1\sigma_n^2}\Big(\mathbf{B}(c_1)\mathbf{B}^H(c_1)\Big)^{-1}. \tag{60}$$

It is worth mentioning that unlike the multiple source case where it is inevitable to estimate both the signal eigenvalue and noise power, here, we do not need to do this because the constant term $\frac{N(\lambda_1-\sigma_n^2)^2}{\lambda_1\sigma_n^2}$ will be canceled out in (59). Therefore, we rewrite $\mathbf{T}$ by ignoring this term as

$$\hat{\mathbf{T}} = \Big(\mathbf{B}(c_1)\mathbf{B}^H(c_1)\Big)^{-1}. \tag{61}$$

Using the results in Proposition 1, the variance of θ_1 is

$$\begin{aligned}\mathbb{E}\big[|\Delta z_1|^2\big] &\approx \frac{1}{2}\left(\frac{\nu}{2\pi d\cos(\theta_1)}\right)^2 \frac{1}{\mathbf{v}_1^H\mathbf{T}\mathbf{v}}\\ &= \frac{1}{2}\left(\frac{\nu}{2\pi d\cos(\theta_1)}\right)^2 \frac{\lambda_1\sigma_n^2}{N(\lambda_1-\sigma_n^2)^2}\frac{1}{\mathbf{v}_1^H\hat{\mathbf{T}}\mathbf{v}}\\ &= \frac{M\text{SNR}+1}{2\text{SNR}^2}\frac{1}{M^2N}\frac{1}{\mathbf{v}_1^H\hat{\mathbf{T}}\mathbf{v}_1}\end{aligned} \tag{62}$$

where $\mathbb{E}\big[|\Delta z|^2\big]$ is simplified by using the fact that $\mathbf{z}_i$ in (76) and α_i in (77) are all equivalent to 1, and the last equation in (62) holds since $\text{SNR} = \sigma_s^2/\sigma_n^2$ and $\lambda_1 = M\sigma_s^2 + \sigma_n^2$ with $\sigma_s^2 = \mathbb{E}[s(t)s^*(t)]$ being the signal power.

The next step is to calculate $\mathbf{v}_1^H\hat{\mathbf{T}}\mathbf{v}_1$. Recalling that $\mathbf{v}_1 = [1 \ z \ \cdots \ z^{M-2}]^T/\sqrt{M}$, we have $\mathbf{I}_{M-1} = M\text{diag}(\mathbf{v}_1)\text{diag}(\mathbf{v}_1)^H$. Then

$$\begin{aligned}\mathbf{v}_1^H\hat{\mathbf{T}}\mathbf{v}_1 &= M^2\mathbf{v}_1^H\text{diag}(\mathbf{v}_1)\text{diag}(\mathbf{v}_1)^H\hat{\mathbf{T}}\text{diag}(\mathbf{v}_1)\text{diag}(\mathbf{v}_1)^H\mathbf{v}_1\\ &= \frac{1}{M}\mathbf{1}_{M-1}^T\text{diag}(\sqrt{M}\mathbf{v}_1)^H\hat{\mathbf{T}}\text{diag}(\sqrt{M}\mathbf{v}_1)\mathbf{1}_{M-1}\\ &= \frac{1}{M}\mathbf{1}_{M-1}^T\bar{\mathbf{T}}\mathbf{1}_{M-1}\end{aligned} \tag{63}$$

where

$$\bar{\mathbf{T}} = \text{diag}(\sqrt{M}\mathbf{v}_1)^H\hat{\mathbf{T}}\text{diag}(\sqrt{M}\mathbf{v}_1). \tag{64}$$

Since calculating $\bar{\mathbf{T}}$ is not straightforward, instead, we first compute its inverse which has the form of

$$\begin{aligned}\bar{\mathbf{T}}^{-1} &= \text{diag}(\sqrt{M}\mathbf{v}_1)(\mathbf{B}(z)\mathbf{B}^H(z))\text{diag}(\sqrt{M}\mathbf{v}_1)^H\\ &= \text{Toeplitz}\big([2 \ -1 \ \mathbf{0}_{M-3}]^T, [2 \ -1 \ \mathbf{0}_{M-3}]\big)\end{aligned} \tag{65}$$

where $\mathbf{B}(z) = \text{Toeplitz}\big([-z \ \mathbf{0}_{M-2}^T]^T, [-z \ 1 \ \mathbf{0}_{M-2}^T]\big)$. Taking the inverse of (65) yields $\bar{\mathbf{T}}$, whose (m,n) entry is

$$\big[\bar{\mathbf{T}}\big]_{m,n} = \begin{cases}\dfrac{n(M-m)}{M}, & 1 \le n \le m \le M-1\\ \dfrac{m(M-n)}{M}, & 1 \le m < n \le M-1.\end{cases} \tag{66}$$

After some algebraic steps, we obtain

$$\mathbf{v}_1^H\hat{\mathbf{T}}\mathbf{v}_1 = \frac{M^2-1}{12}. \tag{67}$$

Combining (62) and (67), the variance of $\hat{\theta}_1$ for $N \to \infty$ becomes

$$\mathbb{E}[(\Delta\theta_1)^2] \approx \left(\frac{\nu}{2\pi d\cos(\theta_1)}\right)^2 \frac{M\text{SNR}+1}{\text{SNR}^2}\frac{6}{M^2N(M^2-1)} \tag{68}$$

which is exactly the CRB [33].

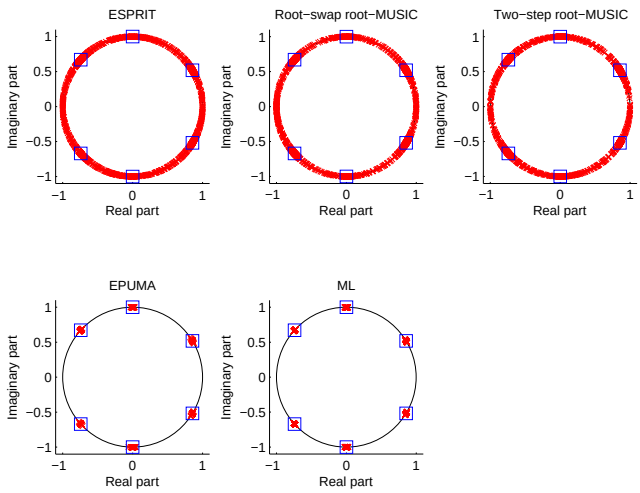

Fig. 3. RMSE performance versus SNR when $N = 2$ and six uncorrelated signals with $\theta = [-50°, -30°, -10°, 10°, 30°, 50°]$. The '×' stands for the estimates and □ stands for the true values.

V. Simulation Results

To illustrate the performance of the EPUMA scheme and to validate the analytical error expression in (47), simulation examples are presented in this section for several representative cases. Meanwhile, the stochastic ML [33], root-swap root-MUSIC [10], two-step root-MUSIC [10] and ESPRIT [4] algorithms are employed for performance comparison. Note that the EPUMA approach with $P = K + 1$ is initialized by $\mathbf{W}_{\text{init}}$ in (43) and then refined by two iterations. For the two-step root-MUSIC method, the user-determined factor γ is estimated by searching from 0 to 1 with step 0.1. In our simulations, the signals are assumed to be Gaussian with equal power, impinging upon a ULA consisting of $M = 10$ omnidirectional sensors with interelement spacing $d = 0.5\nu$. The noise is assumed to be a white Gaussian process with mean zero and variance σ_n^2. The SNR is equal for all the sources.

In the first example, we consider a severely sample-starved scenario where there are $K = 6$ uncorrelated sources from $\theta_1 = -50°$, $\theta_2 = -30°$, $\theta_3 = -10°$, $\theta_4 = 10°$, $\theta_5 = 30°$ and $\theta_6 = 50°$ but only $N = 2$ snapshots are available, so that we have $N < K$. The SNR is 20 dB. Fig. 3 plots the real and imaginary parts of $e^{j\pi \sin(\hat{\theta}_i)}$ under 200 independent tests. It is seen that ESPRIT, root-swap root-MUSIC and two-step root-MUSIC fail to resolve the six signals, while the EPUMA as well as the ML method successfully determine all of them.

In the second example, we compare the RMSE performance versus SNR. All the following results are averaged from 2000 independent runs using a computer with 2.6 GHz dual-core Intel i5 processor and 8 GB RAM. We also examine performance in terms of the probability of DOA resolution, where the DOAs are considered to be resolved if the following is satisfied

$$|\hat{\theta}_i - \theta_i| < \frac{\Delta\theta}{2}, \ i = 1, 2, 3 \tag{69}$$

where $\Delta\theta = \min\{|\theta_m - \theta_n|, 1 \leq n < m \leq 3\}$. The analytical variance of EPUMA is calculated through (47). Fig. 4 is plotted under $K = 3$ coherent signals with DOAs $\theta_1 = 1°$, $\theta_2 = 8°$ and $\theta_3 = 35°$. The number of samples is $N = 50$. Since the two-swap root-MUSIC, two-step root-MUSIC and ESPRIT cannot handle coherent signals, we adopt the well-known FBSS technique [13] to help them work properly. It is seen in Fig. 4 that the performance of EPUMA is very close to the ML estimator, and it outperforms the two-swap root-MUSIC, two-step root-MUSIC and ESPRIT algorithms by a considerable margin. When SNR > -2 dB, the EPUMA and ML schemes almost attain the CRB. We can also observe that the two-step root-MUSIC improves the threshold performance a lot, while the ESPRIT suffers severe performance degradation for SNR < -2 dB. Although the FBSS helps to remove the coherency, due to the loss of DOF, the root-MUSIC and ESPRIT methods are still inferior to the proposed one. Furthermore, it should be noted that although the ML estimator provides the optimal performance, it is typically computationally very intensive because of the need to solve a hard nonconvex multidimensional optimization problem (in fact obtaining the ML solution cannot be guaranteed). Among the four competitors, the ML is the most computationally intensive method[5], while the ESPRIT is the fastest one but with the worst performance. The CPU times of the EPUMA, two-swap and two-step root-MUSIC algorithms are 0.0042s, 0.0022s and 0.0061s, respectively. It is obvious that the EPUMA is computationally simpler than the two-step root-MUSIC but a little bit intensive than the two-swap root-MUSIC. In Fig. 5, we find that the ML followed by the EPUMA feature the highest probability of resolution when SNR is lower than -5 dB, and the four algorithms can resolve all the DOAs with probability 100% when SNR is higher than 0 dB. Although the estimation accuracy of the two-step root-MUSIC is a little bit inferior to that of the two-swap root-MUSIC when SNR < -5 dB, the former has a higher probability of resolution than the latter.

We next study the performance as a function of N. Here, the number of samples is varied from 10 to 1000. All the parameters are the same as Fig. 4 except that the SNR is fixed at a relatively low value of -5 dB. It is seen in Fig. 6 that when $N < 50$, the ML has the best threshold performance, while the EPUMA is somewhat inferior to the ML method. With N increasing, our algorithm converges to its theoretical performance. However, the RMSEs of ESPRIT, root-swap and two-step root-MUSIC estimators cannot reach the CRB even for $N = 1000$. Fig. 7 shows the corresponding results as Fig. 6.

We now consider a special case where there is only one signal with $\theta = 0°$. The sample size is $N = 2$. Since there is no coherent signal, for the two-step root-MUSIC and ESPRIT, we employ the SCM for DOA estimation. As is shown in Fig. 8, the EPUMA has better threshold performance than the root-swap and two-step root-MUSIC, and its theoretical RMSE curve aligns with the CRB, which verifies the correctness of

[5]The computational complexity of the ML estimator is about $\mathcal{O}((M^3 \times \text{length of search region})^K)$, which is typically a multidimensional searching procedure and thus is much more computationally intensive than most of the subspace based algorithms.

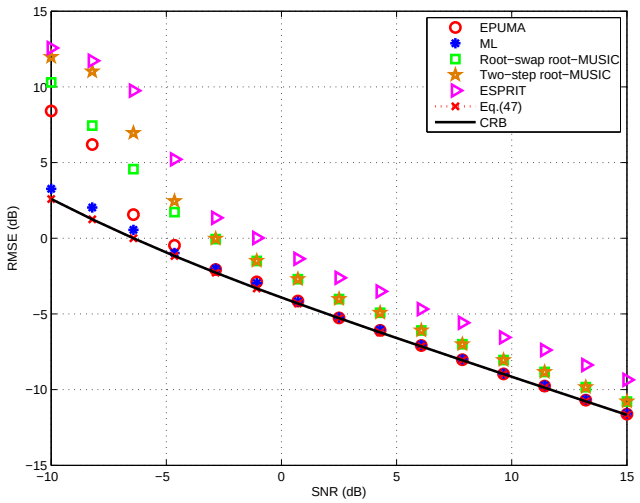

Fig. 4. RMSE performance versus SNR when $N = 50$ and three coherent signals with $\theta = [1°, 8°, 35°]$.

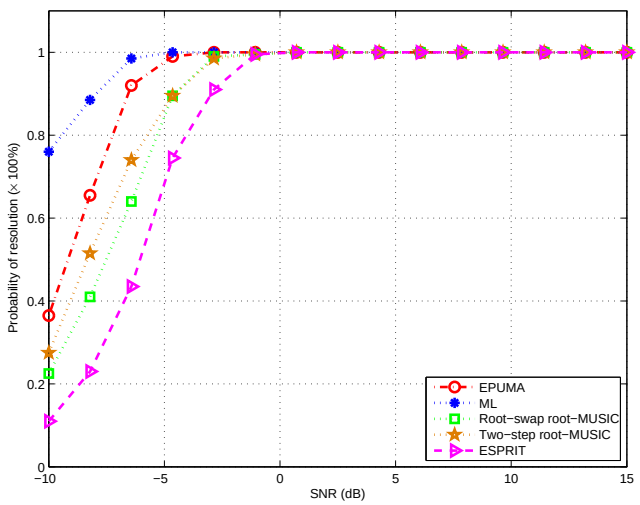

Fig. 5. Probability of resolution versus SNR when $N = 50$ and three coherent signals with $\theta = [1°, 8°, 35°]$

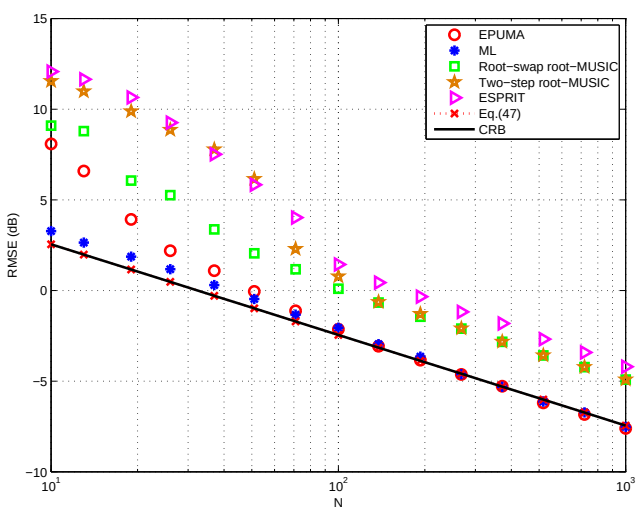

Fig. 6. RMSE performance versus N when SNR $= -5$ dB and three coherent signals with $\theta = [1°, 8°, 35°]$.

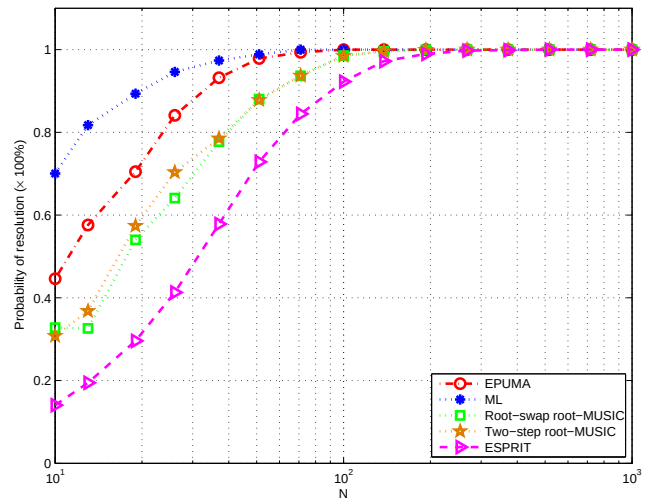

Fig. 7. Probability of resolution versus N when SNR $= -5$ dB and three coherent signals with $\theta = [1°, 8°, 35°]$.

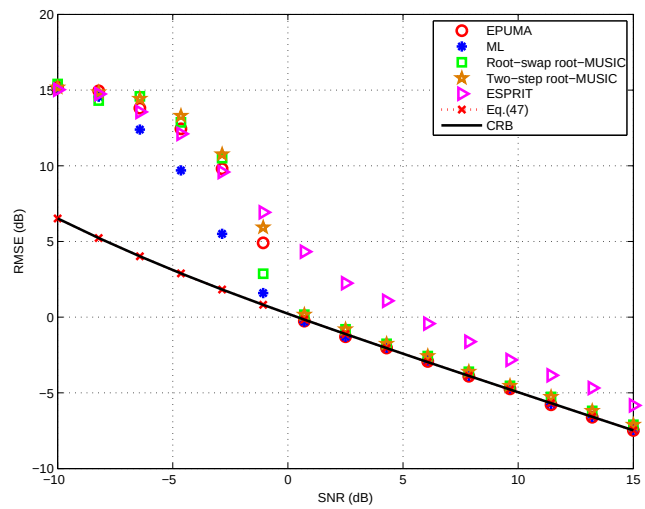

Fig. 8. RMSE performance versus SNR when $N = 2$ and one source with $\theta = 0°$.

our analysis in Section IV-B.

Finally, Fig. 9 shows the computational time of EPUMA, root-swap root-MUSIC, two-step root-MUSIC and ESPRIT as a function of M. It is seen that the ESPRIT is the computationally simplest one among the four competitors. Note that the CPU time of EPUMA is almost independent of M, while the computational time of the two root-MUSIC algorithms increases as M increasing. Specifically, when $M \geq 15$, the EPUMA becomes much faster than the root-swap root-MUSIC. This is because the latter determines final DOA estimates by dividing $(M-1)$ DOA candidates into $(M-1)!/(K!(M-K-1)!)$ different possible combinations and then picking up one that minimizes the stochastic ML cost function. Thus, the complexity of root-swap root-MUSIC is about $\mathcal{O}(M^2N + M^3 \times (M-1)!/(K!(M-K-1)!))$. When $G(G \geq K)$ is large, we have $(M-1)!/(K!(M-K-1)!) \gg G$, which means that the computational complexity of root-swap root-MUSIC is higher than that of the EPUMA.

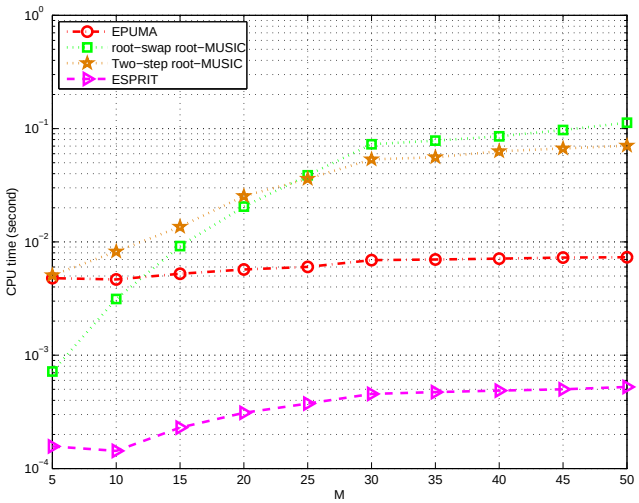

Fig. 9. Computational time versus M when $N = 50$ and $K = 3$.

VI. Conclusion

An EPUMA algorithm for DOA estimation has been devised here, along with its asymptotic performance analysis leading to closed-form mean square error expressions in the large sample regime. The EPUMA technique provides reliable performance when the number of samples is small, even for $N < K$. Moreover, the EPUMA can deal with coherent signals. Computer simulations confirm our theoretical derivations, indicating that the EPUMA approach outperforms many other subspace based DOA estimators, especially for small sample scenarios.

Appendix A
Proof of Proposition 1

As the quantity of interest is θ_i, we need to find the relationship between the error in θ_i and the error in $\mathbf{z}_i$. Noticing that $z_i = e^{j2\pi \sin(\theta_i)\nu/d}$ and performing the first-order Taylor series expansion, we have

$$\Delta\theta_i \approx \frac{\nu}{2\pi d\cos(\theta_i)} \cdot \frac{\Delta z_i}{j z_i}. \tag{70}$$

To ensure $\Delta\theta_i$ a real quantity, we set

$$\Delta\theta_i = \frac{1}{2}(\Delta\theta_i + \Delta\theta_i^*). \tag{71}$$

After some algebraic manipulations, we obtain

$$\mathbb{E}[(\Delta\theta_i)^2] \approx \frac{1}{2}\left(\frac{\nu}{2\pi d\cos(\theta_i)}\right)^2 \cdot \Big(\mathbb{E}\big[|\Delta z_i|^2\big] - \mathrm{Re}\big(\mathbb{E}\big[(\Delta z_i)^2\big](z_i^*)^2\big)\Big). \tag{72}$$

Expanding (7) yields

$$z^P + c_1 z^{P-1} + \cdots + c_P = 0. \tag{73}$$

All the z_i corresponding to the true DOAs should satisfy (73). Thus, by using the first-order approximation, we have

$$\mathbf{z}_i^T \Delta\mathbf{c} + \alpha_i \Delta z_i \approx 0 \tag{74}$$

where

$$\Delta\mathbf{c} = [\Delta c_1 \ \cdots \ \Delta c_P]^T \tag{75}$$

$$\mathbf{z}_i = [z_i^{P-1} \ \cdots 1]^T \tag{76}$$

$$\alpha_i = P z_i^{P-1} + (P-1)c_1 z_i^{P-2} + \cdots + c_{P-1}. \tag{77}$$

Then we get

$$\Delta z_i \approx -\frac{\mathbf{z}_i^T \Delta\mathbf{c}}{\alpha_i}. \tag{78}$$

The variance of $\mathbf{z}_i$ can be expressed as

$$\mathbb{E}\big[|\Delta z_i|^2\big] \approx \frac{\mathbf{z}_i^T \mathbb{E}\big[\Delta\mathbf{c}\Delta\mathbf{c}^H\big]\mathbf{z}_i^*}{|\alpha_i|^2}. \tag{79}$$

Let

$$f(\mathbf{c}) = (\hat{\mathbf{F}}\mathbf{c} - \hat{\mathbf{g}})^H \mathbf{W}(\hat{\mathbf{F}}\mathbf{c} - \hat{\mathbf{g}}). \tag{80}$$

For sufficiently high SNR, we are able to approximate the derivative of $f(\hat{\mathbf{c}})$ using the first- and second-order terms in its Taylor series expansion about the true value $\mathbf{c}$ as [35]

$$0 = f'(\hat{\mathbf{c}}) \approx f'(\mathbf{c}) + f''(\mathbf{c})\Delta\mathbf{c} \tag{81}$$

where $\Delta\mathbf{c} = \hat{\mathbf{c}} - \mathbf{c}$. The first and second derivatives of $f(\mathbf{c})$ with respective to $\mathbf{c}$ are

$$\begin{aligned} f'(\mathbf{c}) &= 2\hat{\mathbf{F}}^H \mathbf{W}(\hat{\mathbf{F}}\mathbf{c} - \hat{\mathbf{g}}) \\ &= 2(\mathbf{F} + \Delta\mathbf{F})^H \mathbf{W}\big((\mathbf{F} + \Delta\mathbf{F})\mathbf{c} - (\mathbf{g} + \Delta\mathbf{g})\big) \\ &\approx 2\mathbf{F}^H \mathbf{W}\big(\mathbf{I}_K \otimes \mathbf{B}(\mathbf{c})\big)\Delta\mathbf{u}_s \end{aligned} \tag{82}$$

$$\begin{aligned} f''(\mathbf{c}) &= 2(\hat{\mathbf{F}}\mathbf{W}\hat{\mathbf{F}}) \\ &\approx 2(\mathbf{F}^H\mathbf{W}\mathbf{F} + \mathbf{F}^H\mathbf{W}\Delta\mathbf{F} + \Delta\mathbf{F}^H\mathbf{W}\mathbf{F}). \end{aligned} \tag{83}$$

Thus, we have

$$\begin{aligned} \mathbb{E}\big[\Delta\mathbf{c}\Delta\mathbf{c}^H\big] &\approx \mathbb{E}\big[(f''(\mathbf{c}))^{-1} f'(\mathbf{c}) \cdot \big((f''(\mathbf{c}))^{-1} f'(\mathbf{c})\big)^H\big] \\ &= \big(\mathbb{E}\big[f''(\mathbf{c})\big]\big)^{-1} \mathbb{E}\big[f'(\mathbf{c})(f'(\mathbf{c}))^H\big] \Big(\mathbb{E}\big[f''(\mathbf{c})\big]^{-1}\Big)^H \\ &\approx (\mathbf{F}^H\mathbf{W}\mathbf{F})^{-1} \end{aligned} \tag{84}$$

where

$$\mathbb{E}\big[f'(\mathbf{c})(f'(\mathbf{c}))^H\big] \approx 4(\mathbf{F}^H\mathbf{W}\mathbf{F}) \tag{85}$$

$$\mathbb{E}\big[f''(\mathbf{c})\big] \approx 2(\mathbf{F}^H\mathbf{W}\mathbf{F}). \tag{86}$$

Plugging (84) into (79) produces

$$\mathbb{E}\big[|\Delta z_i|^2\big] \approx \frac{\mathbf{z}_i^T \big(\mathbf{F}^H\mathbf{W}\mathbf{F}\big)^{-1}\mathbf{z}_i^*}{|\alpha_i|^2}. \tag{87}$$

The next step is to compute $\mathbb{E}\big[(\Delta z_i)^2\big]$. It follows from (78) that

$$\mathbb{E}\big[(\Delta z_i)^2\big] \approx \frac{\mathbf{z}_i^T \mathbb{E}\big[\Delta\mathbf{c}\Delta\mathbf{c}^T\big]\mathbf{z}_i}{\alpha_i^2} \tag{88}$$

where

$$\begin{aligned} \mathbb{E}\big[\Delta\mathbf{c}\Delta\mathbf{c}^T\big] \approx\ & (\mathbf{F}^H\mathbf{W}\mathbf{F})^{-1}\mathbf{F}^H\mathbf{W}\big(\mathbf{I}_K \otimes \mathbf{B}(\mathbf{c})\big)\mathbb{E}\big[\Delta\mathbf{u}_s\Delta\mathbf{u}_s^T\big] \\ & \big(\mathbf{I}_K \otimes \mathbf{B}(\mathbf{c})\big)^T \mathbf{W}^T\mathbf{F}^*(\mathbf{F}^H\mathbf{W}\mathbf{F})^{-T} \end{aligned} \tag{89}$$

With the results in [29]-[31], we have

$$\mathbb{E}\big[\Delta\mathbf{u}_i\Delta\mathbf{u}_j^T\big] \approx -\frac{\lambda_i\lambda_j}{N(\lambda_i - \lambda_j)^2}\mathbf{u}_j\mathbf{u}_i^T(1 - \delta_{ij}) \tag{90}$$

which results in

$$\mathbb{E}\big[\Delta\mathbf{u}_s\Delta\mathbf{u}_s^T\big] \approx \begin{bmatrix} \mathbf{0}_M & \mathbb{E}\{\Delta\mathbf{u}_1\Delta\mathbf{u}_2^T\} & \cdots & \mathbb{E}\big[\Delta\mathbf{u}_1\Delta\mathbf{u}_K^T\big] \\ \mathbb{E}\big[\Delta\mathbf{u}_2\Delta\mathbf{u}_1^T\big] & \mathbf{0}_M & \cdots & \mathbb{E}\big[\Delta\mathbf{u}_2\Delta\mathbf{u}_K^T\big] \\ \vdots & \vdots & \ddots & \vdots \\ \mathbb{E}\big[\Delta\mathbf{u}_K\Delta\mathbf{u}_1^T\big] & \mathbb{E}\big[\Delta\mathbf{u}_K\Delta\mathbf{u}_2^T\big] & \cdots & \mathbf{0}_M \end{bmatrix} \tag{91}$$

Utilizing $\mathbf{B}(\mathbf{c})\mathbf{u}_i = \mathbf{0}_{M-P}, i = 1, \cdots, P$, again, we find that (89) is reduced to be a $K \times K$ zero matrix, such that

$$\mathbb{E}\big[(\Delta z_i)^2\big] \approx 0. \tag{92}$$

Therefore, (72) is then simplified as

$$\mathbb{E}[(\Delta\theta_i)^2] \approx \frac{1}{2}\left(\frac{\nu}{2\pi d\cos(\theta_i)}\right)^2 \mathbb{E}\big[|\Delta z_i|^2\big]. \tag{93}$$

Substituting (87) into (93) proves Proposition 1.

References

[1] R. O. Schmidt, Multiple emitter location and signal parameter estimation, *IEEE Trans. Antennas and Propagation*, vol. AP-34, no. 3, pp. 276-280, 1986

[2] P. Vallet, X. Mestre and P. Loubaton, "Performance analysis of an improved MUSIC DoA estimator," *IEEE Trans. Signal Process.*, vol. 63, no. 23, pp. 6407-6422, 2015.

[3] J. M. Kim, O. K. Lee and J. C. Ye, "Compressive MUSIC: Revisiting the link between compressive sensing and array signal processing," *IEEE Trans. Information Theory*, vol. 58, no. 1, pp. 278-301, 2012.

[4] R. Roy and T. Kailath, "ESPRIT - Estimation of signal parameters via rotational invariance techniques," *IEEE Trans. Acoust., Speech, Signal Process.*, vol. 37, no. 7, 1989.

[5] C. Qian, L. Huang, and H. C. So, "Computationally efficient ESPRIT algorithm for direction-of-arrival estimation based on Nyström method," *Signal Process.*, vol.94, no.1, pp.74-80, 2014.

[6] X. Yuan, "Estimating the DOA and the polarization of a polynomial-phase signal using a single polarized vector-sensor," *IEEE Trans. Signal Process.*, vol. 60, no. 3, pp. 1270-1282, 2012.

[7] A. B. Gershman and J. F. Bohme, "A pseudo-noise resampling approach to direction of arrival estimation using estimator banks," *Proceedings of the 9th IEEE SP Workshop on Statistical Signal and Array Process.*, pp.244-247, Portland, OR, USA, 1998.

[8] C. Qian, L. Huang, and H. C. So, "Improved unitary root-MUSIC for DOA estimation based on pseudo-noise resampling," *IEEE Signal Processing Letters*, vol. 21, no. 2, pp. 140-144, 2014.

[9] A. B. Gershman and M. Haardt, "Improving the performance of unitary ESPRIT via pseudo-noise resampling," *IEEE Trans. Signal Process.*, vol. 47, no. 8, pp. 2305-2308, 1999.

[10] M. Shaghaghi and S. A. Vorobyov, "Subspace leakage analysis and improved DOA estimation with small sample size," *IEEE Trans. Signal Process.*, vol. 63, no. 12, pp. 3251-3265, 2015.

[11] A. B. Gershman and P. Stoica, "New MODE-based techniques for direction finding with an improved threshold performance," *Signal Process.*, vol. 76, no. 3, pp. 221-235, 1999.

[12] T. J. Shan, M. Wax and T. Kailath, "On spatial smoothing for direction-of-arrival estimation of coherent signals," *IEEE Trans. Acoust. Speech, Signal Process.*, vol. 33, no. 4, pp. 806-811, 1985.

[13] S. U. Pillai and B. H. Kwon, "Forward/backward spatial smoothing techniques for coherent signal identification," *IEEE Trans. Acoust., Speech, Signal Process.*, vol. 37, no. 1, pp. 8-15, 1989.

[14] H. C. So, F. K. W. Chan, W. H. Lau, and C. F. Chan, "An efficient approach for two-dimensional parameter estimation of a single-tone," *IEEE Trans. Signal Process.*, vol. 58, no. 4, pp. 1999-2009, 2010.

[15] C. Qian, L. Huang, H. C. So, N. D. Sidiropoulos and J. Xie, "Unitary PUMA algorithm for estimating the frequency of a complex sinusoid," *IEEE Trans. Signal Process.*, vol. 63, no. 20, pp. 5358-5368, 2015.

[16] F. K. W. Chan, H. C. So and W. Sun, "Subspace approach for two-dimensional parameter estimation of multiple damped sinusoids," *Signal Process.*, vol. 92, no. 9, pp. 2172-2179, 2012.

[17] D. W. Tufts and R. Kumaresan, "Singular value decomposition and improved frequency estimation using linear prediction," *IEEE Trans. Acoustics, Speech and Signal Process.*, vol. 30, no. 4, pp. 671-675, 1982.

[18] D. W. Tufts and R. Kumaresan, "Estimation of frequencies of multiple sinusoids: Making linear prediction perform like maximum likelihood," *Proceedings of the IEEE*, vol. 70, no. 9, pp. 975-989, 1982.

[19] V. F. Pisarenko, "The retrieval of harmonics by linear prediction," *Geophys. J. R. Astron. Soc.*, vol. 33, pp. 347366, 1973.

[20] H. Akaike, "A new look at the statistical model identification," *IEEE Trims. Automat. Contr.*, vol. AC-19, pp. 716-723, 1974.

[21] M. Wax and T. Kailath, "Detection of signals by information theoretic criteria," *IEEE Trans. Acoust., Speech, Signal Process.*, vol. 33, no.2, pp. 387-392, 1985.

[22] M. Wax, "Detection and localization of multiple sources via the stochastic signals model," *IEEE Trans. Signal Process.*, vol. 39, no. 11, pp. 2450-2456, 1991.

[23] L. Huang, C. Qian, H.C. So and J. Fang, "Source enumeration for large array using shrinkage-based detectors with small samples," *IEEE Trans. Aerospace and Electronic Systems*, vol. 51, no. 1, pp. 334-357, 2015.

[24] S. Kritchman and B. Nadler, "Non-parametric detection of the number of signals: Hypothesis testing and random matrix theory," *IEEE Trans. Signal Process.*, vol. 57, no. 10, pp. 3930-3941, 2009.

[25] Y. T. Chan, J. M. M. Lavoie, and J. B. Plant, "A parameter estimation approach to estimation of frequencies of sinusoids," *IEEE Trans. Acoust. Speech, Signal Process.*, vol. ASSP-29, no. 2, pp. 214-219, 1981.

[26] E. Grosicki, K. Abed-Meraim and Y. Hua, "A weighted linear prediction method for near-field source localization," *IEEE Trans. Signal Process.*, vol. 53, no. 10, pp. 3651-3660, 2005.

[27] A. Gorokhov, P. Loubaton, and E. Moulines, "Second order blind equalization in multiple input multiple output FIR systems: A weighted least squares approach," in *Proc. Int. Conf. Acoust., Speech, Signal Process.*, vol. 5, pp. 2415-2418, Atlanta, 1996.

[28] D. R. Brillinger, *Time Series: Data Analysis and Theory*. New York: Holt, Rinehart and Winston, 1975.

[29] D. J . Jeffries and D. R. Farrier, "Asymptotic results for eigenvector methods," *IEE Proceedings F (Communications, Radar and Signal Process.)*, vol. 132, no. 7, pp. 589-594, 1985.

[30] M. Kaveh and A. J. Barabell, "The statistical performance of the MUSIC and the minimum-norm algorithms in resolving plane waves in noise," *IEEE Trans. Acoust., Speech, Signal Process.*, vol. ASSP-34. no. 2, pp. 331-341, 1986.

[31] M. Kaveh and A. J. Barabell, "Corrections to "The statistical performance of the MUSIC and the minimum-norm algorithms in resolving plane waves in noise"," *IEEE Trans. Acoust., Speech. Signal Process.*. vol. ASSP-34, no. 3, pp. 633, 1986.

[32] P. Stoica and K. C. Sharman, "Maximum likelihood methods for direction-of-arrival estimation," *IEEE Trans. Acoust., Speech, Signal Process.*, vol. 38, pp. 1132-1143, 1990.

[33] P. Stoica and N. Arye, "MUSIC, maximum likelihood, and Cramér-Rao bound," *IEEE Trans. Acoust., Speech. Signal Process.*, vol. 37, no. 5, pp. 720-741, 1989.

[34] G. H. Golub, and C. F. Van Loan, *Matrix Computations*, JHU Press, 2012.

[35] H. C. So, Y. T. Chan, K. C. Ho and Y. Chen, "Simple formulas for bias and mean square error computation," *IEEE Signal Processing Magazine*, vol. 30, no. 4, pp. 162-165, 2013.

Cheng Qian was born in Deqing, Zhejiang, China. He received the B.E. degree in communication engineering from Hangzhou Dianzi University, Hangzhou, China, in 2011, and M.E. degree in communication and information engineering from Harbin Institute of Technology (HIT), China, in 2013.

Since September 2013, he has been working towards the Ph.D. degree in the field of information and communication engineering at HIT. In addition, he is currently a joint Ph.D. working with the Signal and Tensor Analytics Research (STAR) group at Department of Electrical and Computer Engineering, University of Minnesota. His research interests are in phase retrieval and array signal processing.

Lei Huang (M'07-SM'14) was born in Guangdong, China. He received the B.Sc., M.Sc., and Ph.D. degrees in electronic engineering from Xidian University, Xian, China, in 2000, 2003, and 2005, respectively.

From 2005 to 2006, he was a Research Associate with the Department of Electrical and Computer Engineering, Duke University, Durham, NC. From 2009 to 2010, he was a Research Fellow with the Department of Electronic Engineering, City University of Hong Kong and a Research Associate with the Department of Electronic Engineering, The Chinese University of Hong Kong. From 2011 to 2014, he was a Professor with the Department of Electronic and Information Engineering, Harbin Institute of Technology Shenzhen Graduate School. Since November 2014, he has joined the Department of Information Engineering, Shenzhen University, where he is currently a Chair Professor. His research interests include spectral estimation, array signal processing, statistical signal processing, and their applications in radar and wireless communication systems.

He is currently serving as an Associate Editor for IEEE Transactions on Signal Processing and Digital Signal Processing.

Nikos Sidiropoulos Nicholas D. Sidiropoulos (F'09) received the Diploma in electrical engineering from the Aristotelian University of Thessaloniki, Greece, and M.S. and Ph.D. degrees in electrical engineering from the University of Maryland-College Park, in 1988, 1990 and 1992, respectively.

He served as Assistant Professor at the University of Virginia (1997-1999); Associate Professor at the University of Minnesota-Minneapolis (2000-2002); Professor at the Technical University of Crete, Greece (2002-2011); and Professor at the University of Minnesota-Minneapolis (2011-), where he currently holds an ADC Chair in Digital Technology. His current research focuses primarily on signal and tensor analytics, with applications in cognitive radio, big data, and preference measurement. He received the NSF/CAREER award (1998), the IEEE Signal Processing Society (SPS) Best Paper Award (2001, 2007, 2011), and the IEEE SPS Meritorious Service Award (2010). He has served as IEEE SPS Distinguished Lecturer (2008-2009), and Chair of the IEEE Signal Processing for Communications and Networking Technical Committee (2007-2008). He received the Distinguished Alumni Award of the Department of Electrical and Computer Engineering, University of Maryland, College Park (2013). He was elected Fellow of EURASIP in 2014.

Hing Cheung So Hing Cheung So (S'90-M'95-SM'07-F'15) was born in Hong Kong. He received the B.Eng. degree from City University of Hong Kong (CityU) and the Ph.D. degree from The Chinese University of Hong Kong (CUHK), both in electronic engineering, in 1990 and 1995, respectively. From 1990 to 1991, he was an Electronic Engineer with the Research and Development Division, Everex Systems Engineering Ltd., Hong Kong. During 1995-1996, he worked as a Postdoctoral Fellow at CUHK. From 1996 to 1999, he was a Research Assistant Professor with the Department of Electronic Engineering, CityU, where he is currently an Associate Professor. His research interests include detection and estimation, fast and adaptive algorithms, multidimensional harmonic retrieval, robust signal processing, source localization, and sparse approximation.

He has been on the editorial boards of IEEE Signal Processing Magazine (2014-), IEEE Transactions on Signal Processing (2010-2014), Signal Processing (2010-), and Digital Signal Processing (2011-). He is also Lead Guest Editor for IEEE Journal of Selected Topics in Signal Processing, special issue on "Advances in Time/Frequency Modulated Array Signal Processing". In addition, he is an elected member in Signal Processing Theory and Methods Technical Committee (2011-) of the IEEE Signal Processing Society where he is chair in the awards subcommittee (2015-). He has been named an IEEE Fellow in recognition of his contributions to spectral analysis and source localization.